Supporting Information for "A 30 Year Time Series of Transient Tracer-based Estimates of Anthropogenic Carbon in the Central Labrador Sea"

L. Raimondi[1], T.Tanhua[2], K. Azetsu-Scott[3], I. Yashayaev[3], D.W.R. Wallace[1]

[1]Department of Oceanography, Dalhousie University, Halifax, Nova Scotia, Canada.

[2]Division of Chemical Oceanography, GEOMAR Helmholtz Centre for Ocean Research Kiel, Kiel, Germany.

[3]Department of Fisheries and Oceans, Canada, Bedford Institute of Oceanography, Dartmouth, Nova Scotia, Canada.

Contents of this file

Additional Supporting Information (Files uploaded separately)

1. Captions for Movie S1

S1. Δ/Γ

In Figure S1 we show the approach to select the proper Δ/Γ using mean ages from CFC-12 and SF_6 (as described in section 3.3 of the main text). In Table S1 we provide average differences between each Δ/Γ and reference ratio (Δ/Γ=1.8) when applying our

Corresponding author: L. Raimondi, Department of Oceanography, Dalhousie University, Halifax, Nova Scotia, Canada. (Lorenza.Raimondi@dal.ca)

refined TTD method.

S2. Mixed Layer Depth and Water Masses Definitions

S2.1. Mixed Layer Depth

The MLD values used in this study were obtained from an empirical model based on a correlation between convection depths and winter-time weight-averaged cumulative heat losses. In order to account for the effect of ocean preconditioning, the annual heat loss was quantified as a weighted average value obtained from the 5 preceding years. A decreasing weight was attributed from the 1^{st} to the 5^{th} year prior the year of observation (Yashayaev & Loder, 2017). In the figure S2 we show results of MLD from four simulations where the weight attributed to the preceding years was varied. For our CFC-12 saturation calculations, we used the MLD-4 which was the modelled MLD that best matched the observed MLD.

S2.2. Water Masses Definitions

The principal water masses of the central Labrador Sea were here defined both based on σ_2 (LSW and NEADW) and on depth ranges (Surface Water and DSOW). These definitions were introduced in previous studies in the region (e.g. Yashayaev, 2007; Yashayaev & Loder, 2016). In Table S2 we report the limits of each water mass. Because the Labrador Sea Water definition changes over time we also report the σ_2 limit identified for each year for this water mass in table S3.

For comparison purposes we also calculated average C_{ant} concentrations and inventories for the *upper* LSW (uLSW) and *deep* LSW (dLSW) as defined by Stramma et al. (2004)

and used in Rhein, Steinfeldt, Kieke, Stendardo, and Yashayaev (2017). These results are reported in Figure S3 and S4. Although there are some differences between the two water mass definitions, both display a change in the relative contribution of the two layers ventilated in the Labrador Sea to the C_{ant} column inventory at the time when the storage rate was at its lowest (see top and middle panel of Figure S4).

S3. C_{ant} Results Using SF_6 as Tracer to Constrain Mean Ages

S3.1. C_{ant} Estimates Based on Two SF_6 Saturation Reconstructions

As previously mentioned in the main text in section 3.1, we estimated anthropogenic carbon using both CFC-12 and SF_6. We included different scenarios to calculate C_{ant}: constant 100% saturation for both tracers, time varying saturation based on MLR using tracers' saturation observations. For SF_6 we also modelled the time varying saturation applying the regression coefficients obtained from the MLR with CFC-12 data to the atmospheric history of SF_6. We here report results of C_{ant} calculated from these different scenarios.

Compared to assuming a constant 100% saturation, the C_{ant} concentrations obtained using variable saturation of SF_6 modelled with the CFC-12 regression coefficients were on average $\sim 3 \pm 1$ μmol kg^{-1} higher. This difference was found to be even higher when the SF_6 variable saturation was obtained using regression coefficients based on the SF_6 observations (5 ± 1 μmol kg^{-1} higher).

Inventories calculated with 100% saturation of SF_6, were between 10.5 and 15.9 mol m^{-2} lower when compared to results with SF_6 saturation percentage constrained using the CFC-12 regression coefficients. This difference was between 17.2 and 20.1 mol m^{-2} when the constant saturation was compared to results with SF_6 saturations constrained through

the SF_6 regression coefficients instead.

We obtained a rate of increase (C_{ant} storage rate) of 5.8 and 5.2 mol m^{-2} y^{-1} for values calculated using a variable saturation modelled from CFC-12 and SF_6 regression coefficients, respectively. While with the constant 100% saturation assumption the rate of increase was 4.4 mol m^{-2} y^{-1}. The storage rates reported for SF_6 only cover the period between 2012-2016 therefore in Table S4 we also report results of storage rate obtained with CFC-12. The table S4 and Figure S5 show how the use of a refined TTD leads to better agreement of C_{ant} column inventories obtained with CFC-12 and SF_6.

S3.2. C_{ant} Results from Different Δ/Γ

In Figure S6 we report C_{ant} column inventories for central Labrador Sea from 2012 to 2016 as an average for all the Δ/Γ ratios listed in section 3.3 of the main text (dots) together with their standard deviations (shaded area). We found that using SF_6, the average increase in column inventory was between 163.2 and 185.1 mol m^{-2} over the period 2012 and 2016 using saturations based on the CFC-12 regression coefficients, and between 169.3 and 189.0 mol m^{-2} when saturation was based on SF_6.

Comparing the C_{ant} concentrations based on time variable saturations of SF_6 obtained with the two methods described earlier, we found that the percent difference between C_{ant} concentrations calculated with a Δ/Γ=1.8 and all other ratios ranged from a minimum of -7.9 to a maximum of -0.9% when CFC-12-based regression coefficients were applied to model the SF_6 saturation (see Table S5). This range was found to be between -11 and -3.3% when the SF_6-based regression coefficients were used to model the SF_6 saturation instead (see Table S6). The different concentrations obtained from the Δ/Γ ratios pre-

sented here translated into a maximum difference $\sim 2.5\%$ in column inventory.

Caption Movie S1 (uploaded as separate document): Time evolution of C_{ant} obtained from the refined TTD method. The animation shows the C_{ant} section plots along the AR7W line between 1986 and 2016.

Caption Movie S2 (uploaded as separate document): Time evolution of C_{ant} spatial anomaly. The animation shows the C_{ant} spatial anomaly section plots along the AR7W line between 1986 and 2016. The anomaly was calculated as difference between C_{ant} concentrations at every location minus the average C_{ant} concentration calculated from two end-members: the LSW and the NEADW ($\Delta C_{ant(i,t)} = C_{ant(i,t)} - C_{ant(LSW-NEADW,t)}$, where i is the location and t is year and $C_{ant(LSW-NEADW,t)}$ is the annual average C_{ant} concentrations obtained from LSW and NEADW).

Table S1: Average percent difference in C_{ant} concentrations between each Δ/Γ ratio and a Δ/Γ=1.8 (chosen as our reference based on our ratio selection procedure) obtained with CFC-12. Note that these numbers reflect conditions in Labrador Sea therefore these would be different for regions that are characterized by different ventilation pattern.

	Difference with respect to Δ/Γ = 1.8							
	Δ/Γ	Δ/Γ	Δ/Γ	Δ/Γ	Δ/Γ	Δ/Γ	Δ/Γ	Δ/Γ
Year	0.4	0.6	0.8	1.0	1.2	1.4	1.6	2.0
1986	-3.6	-3.0	-2.3	-1.8	-1.2	-0.7	-0.3	0.3
1992	-3.0	-2.8	-2.3	-1.8	-1.3	-0.8	-0.4	0.3
1993	-2.2	-2.0	-1.7	-1.3	-1.0	-0.6	-0.3	0.3
1994	-2.4	-2.1	-1.7	-1.3	-0.9	-0.6	-0.3	0.3
1995	-2.5	-2.2	-1.8	-1.4	-1.0	-0.6	-0.3	0.3
1996	-3.5	-3.0	-2.4	-1.8	-1.3	-0.8	-0.4	0.4
1997	-3.0	-2.6	-2.1	-1.6	-1.1	-0.7	-0.4	0.3
1998	-3.6	-3.0	-2.3	-1.8	-1.2	-0.8	-0.4	0.3
1999	-2.8	-2.3	-1.8	-1.3	-0.9	-0.6	-0.3	0.2
2000	-4.5	-3.6	-2.8	-2.0	-1.4	-0.9	-0.4	0.3
2001	-3.8	-3.0	-2.4	-1.8	-1.2	-0.8	-0.4	0.2
2002								
2003	-4.0	-3.2	-2.5	-1.9	-1.3	-0.8	-0.4	0.3
2004	-3.0	-2.4	-1.9	-1.4	-1.0	-0.6	-0.3	0.2
2005								
2006	-2.6	-2.2	-1.7	-1.3	-0.9	-0.5	-0.3	0.1
2007	-4.2	-3.5	-2.7	-2.0	-1.3	-0.8	-0.4	0.3
2008								
2009								
2010	-3.0	-2.5	-2.0	-1.4	-1.0	-0.6	-0.3	0.2
2011								
2012	-1.0	-1.0	-0.8	-0.6	-0.4	-0.2	-0.1	0.1
2013	-1.8	-1.7	-1.4	-1.0	-0.7	-0.4	-0.2	0.1
2014	-1.2	-1.2	-1.0	-0.7	-0.5	-0.3	-0.1	0.1
2015	-1.5	-1.3	-1.1	-0.8	-0.5	-0.3	-0.1	0.1
2016	-0.7	-0.7	-0.5	-0.4	-0.3	-0.1	-0.1	0.0

Table S2: Water Masses Definitions based on σ_2 and depth. LSW stands for Labrador Sea Water, DIW stand for Deep-Intermidiate Water, NEADW for North East Atlantic Deep Water and DSOW for Denmark Strait Overflow Water. The LSW_{σ_2} is the σ_2 that defines the extent of LSW. These are reported in Table S3.

Water Mass	Depth/σ_2 Range
SURFACE	0-200m
LSW	>200m - LSW_{σ_2}
DIW	LSW_{σ_2}>σ_2<36.96
NEADW	36.96>σ_2 <37.1
DSOW	bottom 200m

Table S3: Inter-annual variability of the LSW σ_2 limit.

Year	LSW_{σ_2}
1986	36.910
1992	36.943
1993	36.952
1994	36.953
1995	36.942
1996	36.931
1997	36.913
1998	36.893
1999	36.870
2000	36.875
2001	36.887
2002	36.885
2003	36.887
2004	36.881
2005	36.868
2006	36.864
2007	36.842
2008	36.874
2009	36.860
2010	36.817
2011	36.823
2012	36.852
2013	36.850
2014	36.860
2015	36.879
2016	36.896

Table S4: Column inventories ($I_{C_{ant}}$; in mol m^{-2}) and storage rates (SR; in mol m^{-2} y^{-1}) of C_{ant} from different scenarios of tracer's saturation: constant 100% saturation of CFC-12 (CFC-$12_{(CS)}$ (100%)), time varying saturation of CFC-12 (CFC-$12_{(VS)}$), constant 100% saturation of SF_6 ($SF_{6(CS)}$ (100%)), time-varying saturation of SF_6 modelled with CFC-12-based regression coefficients ($SF_{6(VS)}$ (CFC-12 Reg)) and with SF_6-based regression coefficients ($SF_{6(VS)}$ (SF_6 Reg)).

	CFC-$12_{(CS)}$ (100%)	CFC-$12_{(VS)}$	$SF_{6(CS)}$ (100%)	$SF_{6(VS)}$ (CFC-12 Reg)	$SF_{6(VS)}$ (SF_6 Reg)
$I_{C_{ant}}$ (1986-2016)	72.3 - 148.6	112.0-181.4	-	-	-
$I_{C_{ant}}$ (2012-2016)	136.5-148.6	158.9-181.4	147.7-165.7	158.2-181.6	164.9-185.8
SR (1986-2016)	2.1	1.8	-	-	-
SR (2012-2016)	2.6	5.3	4.4	5.8	5.2

Table S5: Average percent difference in C_{ant} concentrations between each Δ/Γ ratio and a Δ/Γ=1.8 (chosen as our reference based on our ratio selection procedure) using SF_6 time varying saturation obtained from CFC12-based regression coefficients.

	Difference with respect to Δ/Γ = 1.8							
	Δ/Γ	Δ/Γ	Δ/Γ	Δ/Γ	Δ/Γ	Δ/Γ	Δ/Γ	Δ/Γ
Year	0.4	0.6	0.8	1.0	1.2	1.4	1.6	2.0
2012	-6.6	-5.5	-4.2	-3.1	-2.1	-1.2	-0.6	0.5
2013	-7.9	-6.5	-5.0	-3.6	-2.4	-1.4	-0.6	0.4
2014	-7.1	-5.7	-4.3	-3.1	-2.1	-1.2	-0.5	0.4
2015	-6.1	-4.9	-3.7	-2.6	-1.7	-1.0	-0.4	0.3
2016	-5.3	-4.2	-3.2	-2.3	-1.5	-0.9	-0.4	0.3

Table S6: Average percent difference in C_{ant} concentrations between each Δ/Γ ratio and a Δ/Γ=1.8 (chosen as our reference based on our ratio selection procedure) using SF_6 time varying saturation obtained from SF_6-based regression coefficients.

	Difference with respect to Δ/Γ = 1.8							
	Δ/Γ	Δ/Γ	Δ/Γ	Δ/Γ	Δ/Γ	Δ/Γ	Δ/Γ	Δ/Γ
Year	0.4	0.6	0.8	1.0	1.2	1.4	1.6	2.0
2012	-9.6	-8.6	-7.5	-6.5	-5.6	-4.9	-4.3	-3.4
2013	-11.0	-9.8	-8.5	-7.3	-6.2	-5.3	-4.6	-3.5
2014	-9.6	-8.5	-7.3	-6.2	-5.3	-4.5	-3.8	-2.9
2015	-8.5	-7.6	-6.5	-5.6	-4.8	-4.1	-3.6	-2.8
2016	-7.2	-6.4	-5.5	-4.6	-3.9	-3.3	-2.8	-2.1

References

Rhein, M., Steinfeldt, R., Kieke, D., Stendardo, I., & Yashayaev, I. (2017). Ventilation variability of labrador sea water and its impact on oxygen and anthropogenic carbon: a review. *Philosophical Transactions of the Royal Society A: Mathematical, Physical and Engineering Sciences*, *375*(2102), 20160321.

Stramma, L., Kieke, D., Rhein, M., Schott, F., Yashayaev, I., & Koltermann, K. P. (2004). Deep water changes at the western boundary of the subpolar north atlantic during 1996 to 2001. *Deep Sea Research Part I: Oceanographic Research Papers*, *51*(8), 1033–1056.

Yashayaev, I. (2007). Hydrographic changes in the Labrador Sea, 1960-2005. *Progress in Oceanography*, *73*(3-4), 242–276. doi: 10.1016/j.pocean.2007.04.015

Yashayaev, I., & Loder, J. (2016). Recurrent replenishment of Labrador Sea Water and associated decadal-scale variability. *Journal of Geophysical Research: Oceans*, *121*(11), 8095–8114.

Yashayaev, I., & Loder, J. W. (2017). Further intensification of deep convection in the labrador sea in 2016. *Geophysical Research Letters*, *44*(3), 1429–1438.

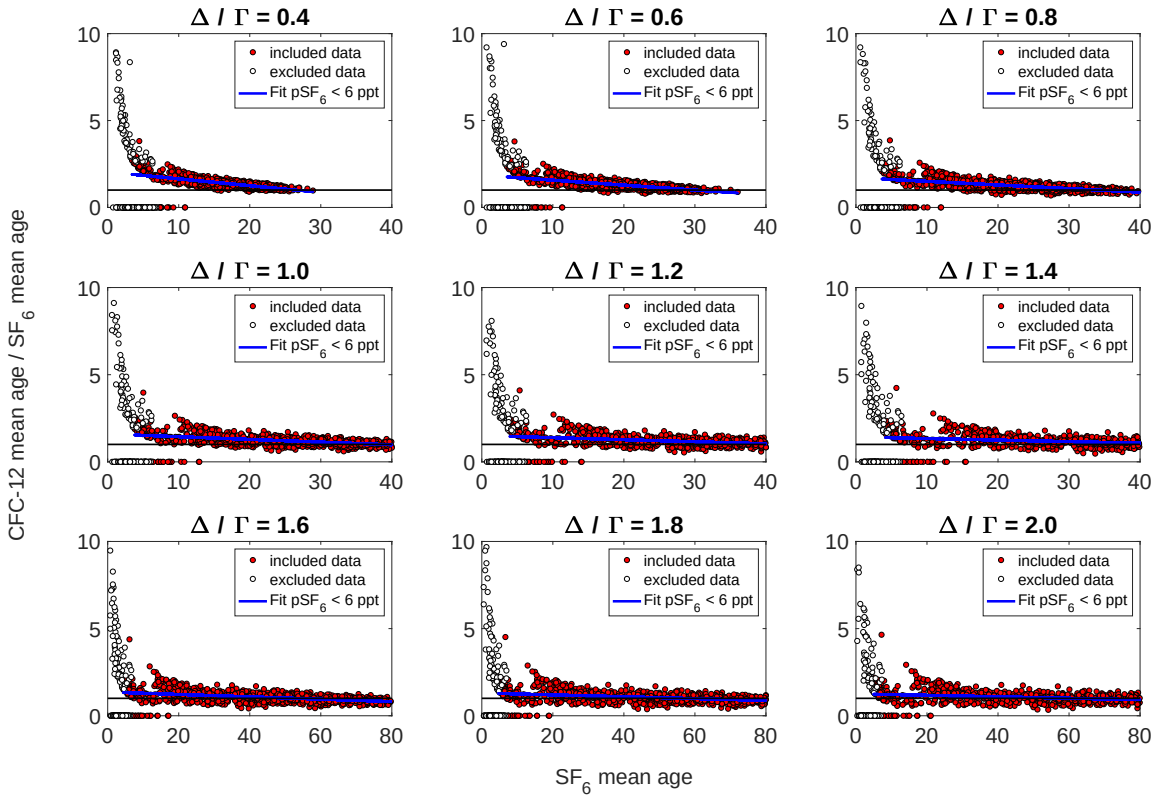

Figure S1. Representation of quantitative selection of the Δ/Γ ratio that better represents physical conditions of the studied area. To objectively select the Δ/Γ, the ratio of mean ages from CFC-12 to mean ages from SF_6 is plotted against mean ages from SF_6, the data points were the SF_6 concentration is <6 ppt were included to obtain a fit of which the slope should be close to 0, the intercept close to 1 and the distance of each data point to the fit should be close to 0.

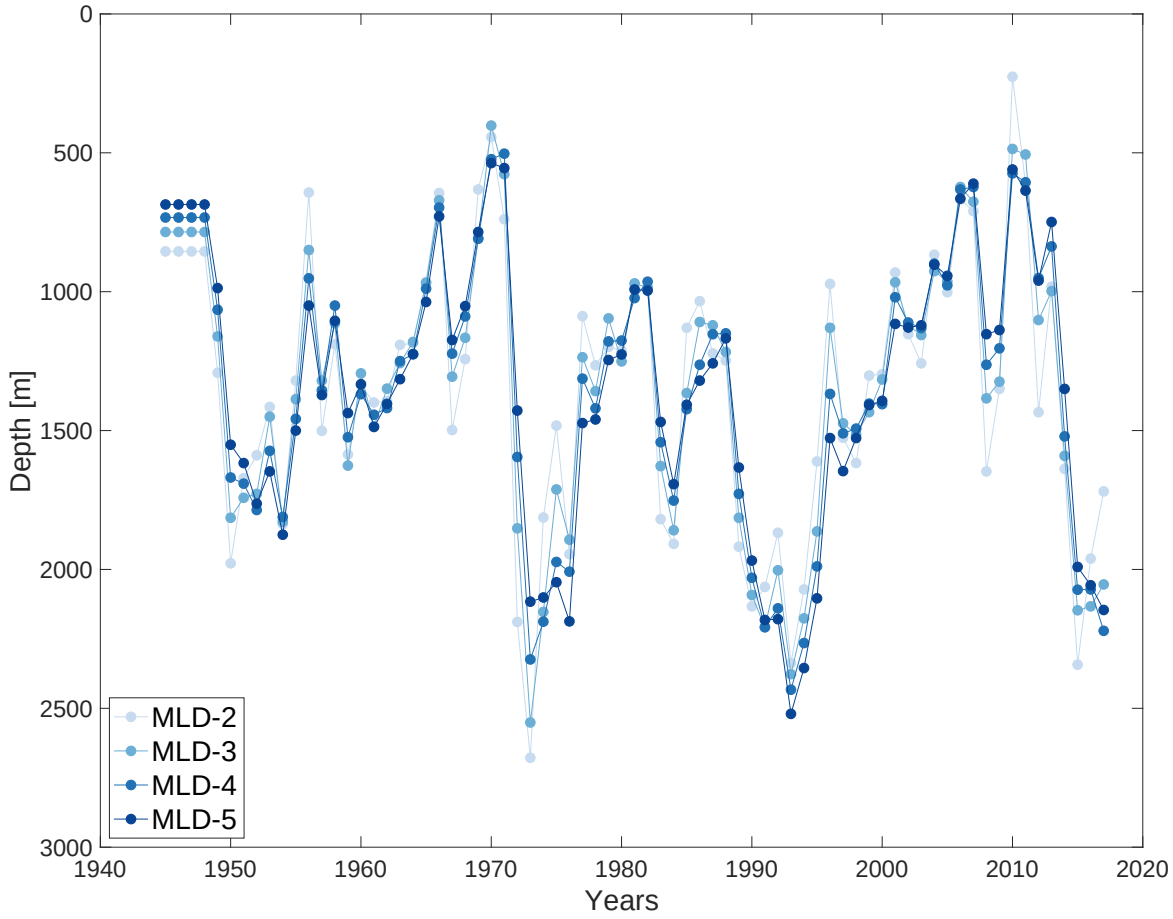

Figure S2. Modelled mixed layer depth from an empirical model. The colours represent the different realizations obtained from the empirical model.

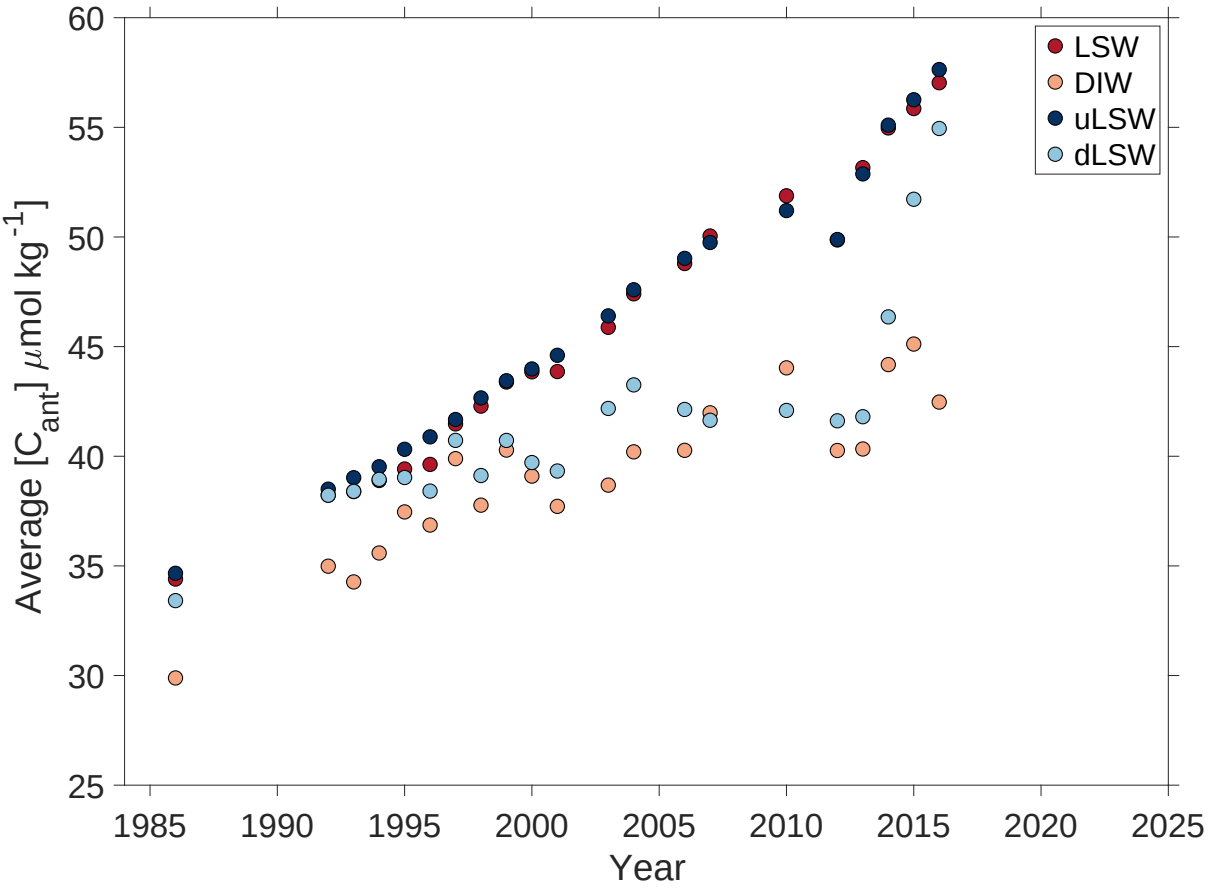

Figure S3. Average C_{ant} concentrations in LSW and DIW as defined in this paper and in uLSW and dLSW as defined in the paper by Rhein et al. (2017).

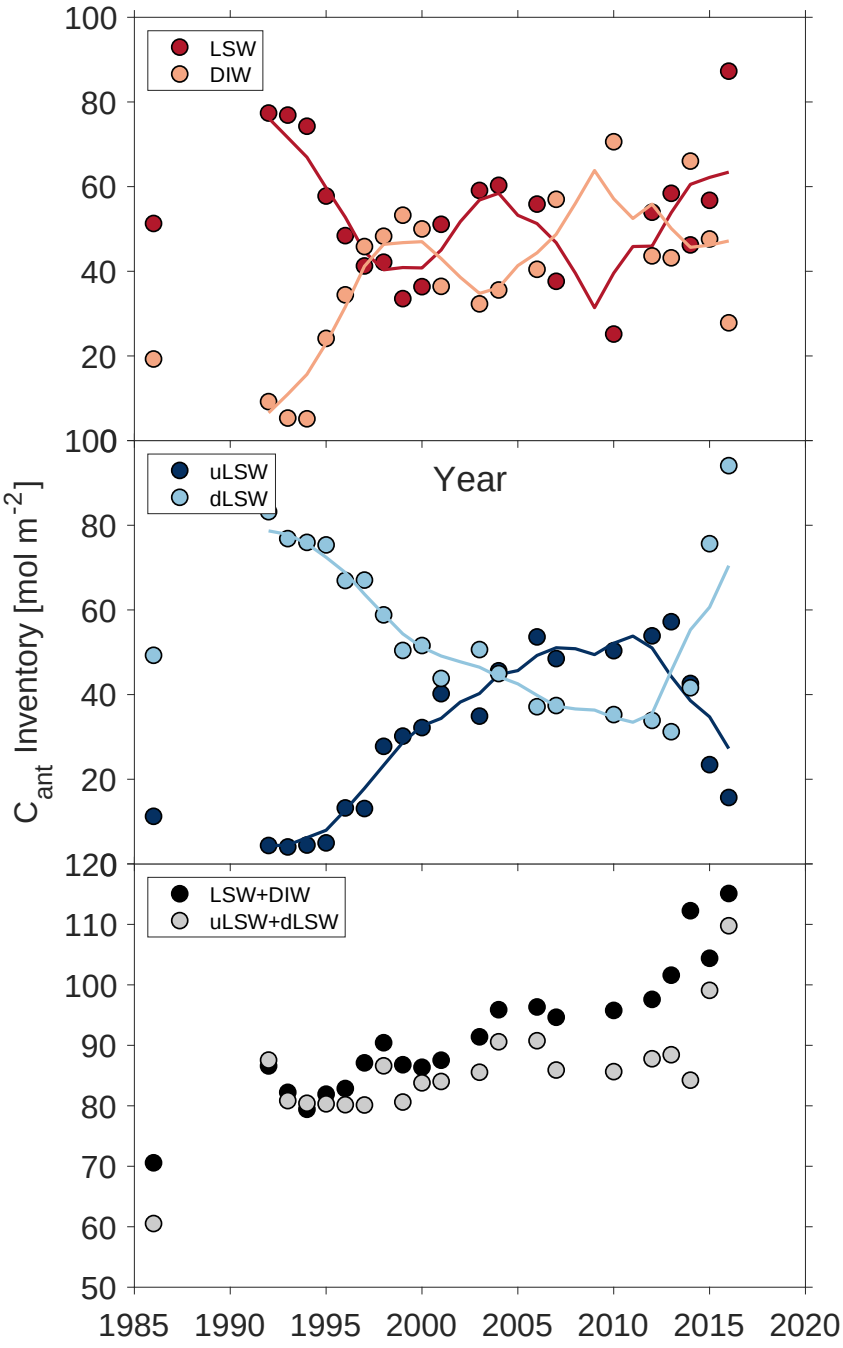

Figure S4. C_{ant} inventories in mol m^{-2} in LSW and DIW defined in this paper (top panel) and in uLSW and dLSW as defined by Stramma et al. (2004) (middle panel). The bottom panel shows the inventory of the sum of the two layers with both definitions (LSW+DIW) and (uLSW+dLSW).

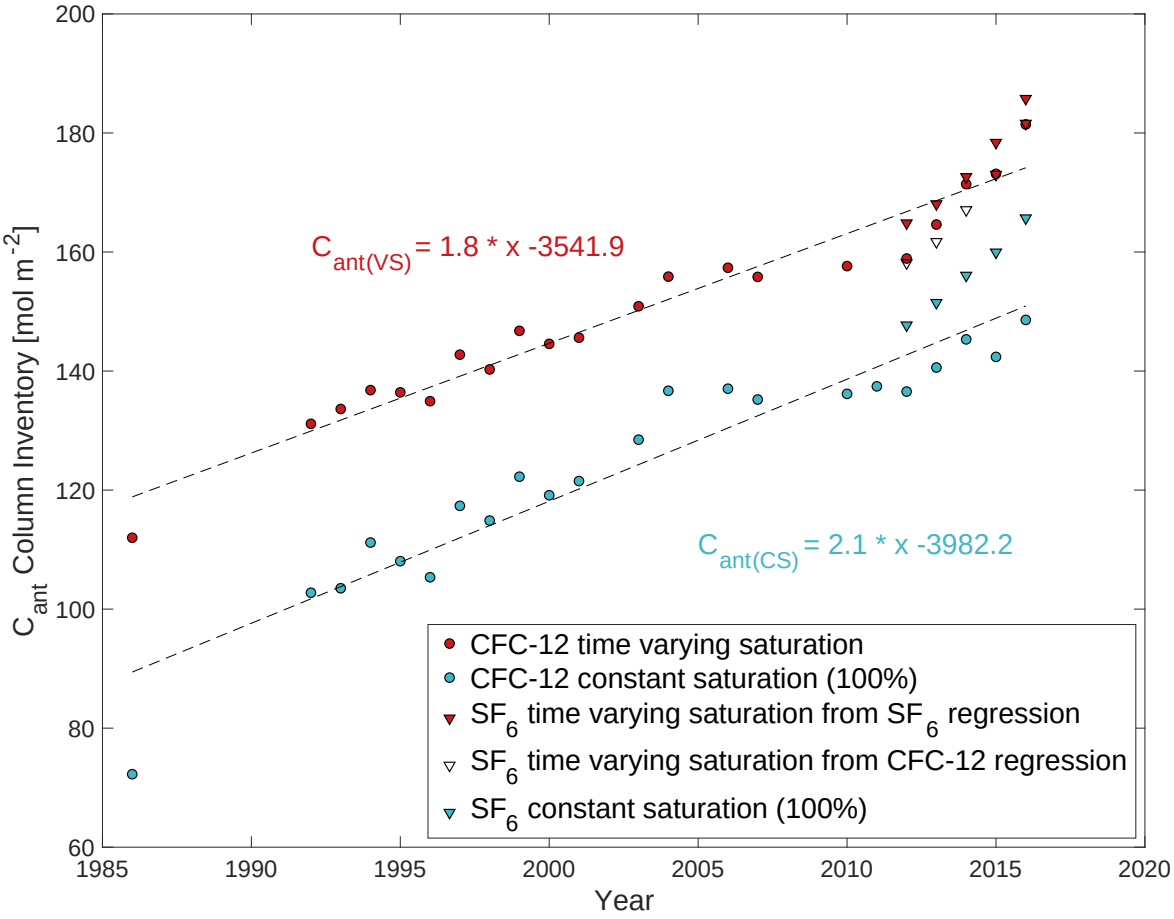

Figure S5. Column inventories of C_{ant} in central Labrador Sea obtained from mean ages calculated using a constant 100% saturation assumption (teal markers) of CFC-12 (dots) and SF_6 (triangles) and the column inventory obtained from our refined TTD methods (red markers). For the SF_6 we also included results obtained with the CFC-12-based regression coefficients applied to the atmospheric history of SF_6 (clear triangles). All calculations of mean ages where performed with Δ/Γ=1.8 for all these C_{ant} estimates.

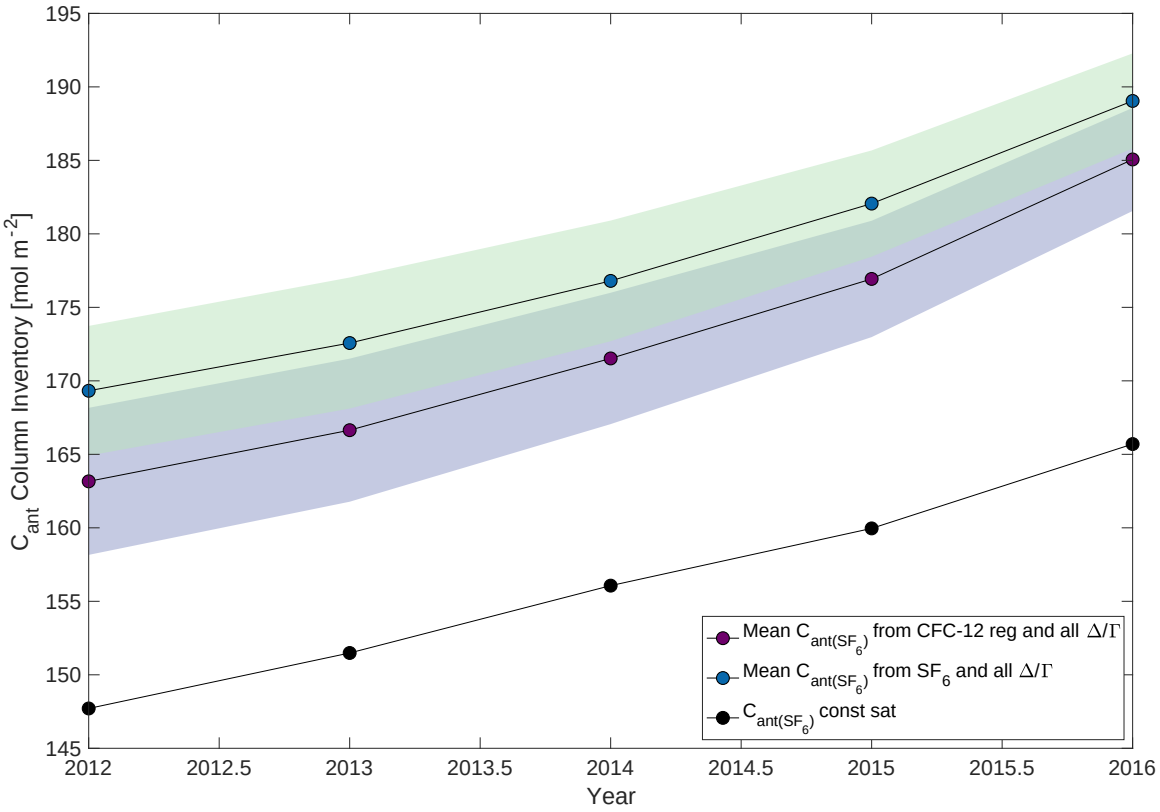

Figure S6. Average column inventories of C_{ant} in central Labrador Sea from 2012 and 2016 using SF_6 data. The data shown were calculated using different Δ/Γ and time variable saturation. For SF_6 we present results using both a time variable saturation modelled with CFC-12-based regression coefficients (purple dots) and with SF_6-based regression coefficients (blue dots). The shaded areas represent the standard deviation obtained from all Δ/Γ. For reference we also report results obtained with constant saturation (black dots).